ELSEVIER

Powder Technology 135–136 (2003) 105–111

POWDER TECHNOLOGY

www.elsevier.com/locate/powtec

Electric field controlled dilute–dense flow transition in granular flow through a vertical pipe

Meiying Hou*, Wei Chen, Tong Zhang, Kunquan Lu

Institute of Physics, Chinese Academy of Sciences, Beijing 100080, China

Received 7 November 2002; received in revised form 27 January 2003; accepted 17 February 2003

Abstract

The flow of granular nickel particles moving down a vertical pipe from a hopper in the presence of a local, horizontal ac electric field is studied. It is found that the flow can be retarded by the electric field, and the retardation depends upon the initial conditions of the flow. If the flow is dilute when passing through the field, there exists a critical voltage V_1, the flow transition from dilute to dense occurs and flow rate is retarded when V is greater than V_1. For $V < V_1$, the steady-state flow rate is practically unaffected. The flow rate decreases abruptly at V_1. Particle aggregations near the top end of the electrodes are observed. A two-dimensional molecular dynamics (MD) simulation is performed. It confirms the aggregation and intermittence of the flow, and the abrupt change in flow rate at the dilute–dense transition. The MD simulation results agree qualitatively well with the experimental observations.

Keywords: Granular materials; Electric fields; Granular flow; Computer simulation of molecular and particle dynamics

1. Introduction

Granular matter is a unique system that exhibits solid-like and fluidlike properties [1,2]. Their peculiar properties have attracted much attention in recent years not only because of its ubiquity in nature and application in technology, but also because of the poor understanding in its basic mechanism [2,3]. Dynamical behavior of granular flow in a vertical pipe is one of the most challenging subjects in the field, and many interesting phenomena have been observed [4–8].

The peculiar properties of granular materials can be attributed to their strong contact interactions and inelastic collisions between particles. Introducing a long-range interaction to compete with these short-range contact forces may provide a new control parameter in elucidating the underlain mechanism. Considering the Electro-rheological (ER) effect of particles in fluids induced by electric field, we are interested in effects of applying an electric field to the granular flow.

Controlled by electric field particle clustering and phase-transition from a granular solid phase to a gas phase were formed and studied by Aranson et al. [9]. Electric field has also been investigated and applied as an electromechanical valve to control the bulk transportation of semiconducting particles such as agricultural seeds [10,11]. In their studies dense-phase flow of dry granular materials is controlled by the applied electric field using two electrodes installed within the flow duct. The interparticle forces generated by the electric field causes the flow to be retarded or halted as the field becomes high enough. Other examples of applying electric field in granular flows are reported such as in the spouted bed [12] to regulate the solid recirculation rate, and in packed and fluidized beds [13] to effectively alter the bed dynamics.

We have recently studied experimentally dilute and dense granular flows down a vertical pipe in the presence of an electric field. Some interesting phenomena such as arch formation and wavelength elongation of a density wave at high enough electric field were observed [14]. We also found that the local electric field was able to retard the downward movement of a dense column of particles (similar to what Ghadiri et al. [11] found in their electromechanical valve), but was ineffective in doing so when the column of the particles was dilute in density [15].

To understand the electric field effects to the dense and dilute flows, we have prepared the flow system in two

* Corresponding author. Tel.: +86-1082649089; fax: +86-1082640224.
E-mail address: mayhou@aphy.iphy.ac.cn (M. Hou).

0032-5910/$ - see front matter © 2003 Elsevier B.V. All rights reserved.
doi:10.1016/S0032-5910(03)00158-X

particular sequences to separate the dilute and dense flows, and found that depending upon the initial flow conditions, the flow was retarded by the applied electric field [16]. For dilute flow, the flow rate does not change until the field voltage is higher than a critical voltage V_1, at which dilute flow transformed to dense flow and retarded by the electric field when V is higher than V_1. For dense flow, the field retards the flow rate monotonically when the voltage is higher than a different voltage V_2, while $V_2 < V_1$ and V_2 is solely determined by the inflow rate. The flow rate of a dense flow decreases with a power law, $Q \sim V^{-1}$. Suppression of the high frequency components in the flow density fluctuation is observed at $V > V_1$. It indicates that aggregation occurs when particles are passing through the electric field. A two-dimensional Molecular Dynamics simulation is performed. Qualitative agreement of the flow rate dependence on the applied voltage and the suppression of the high frequency components at $V > V_1$ are achieved.

2. Experimental results

A schematic diagram of the experimental setup is shown in Fig. 1. In our experiments, two sizes of nickel particles,

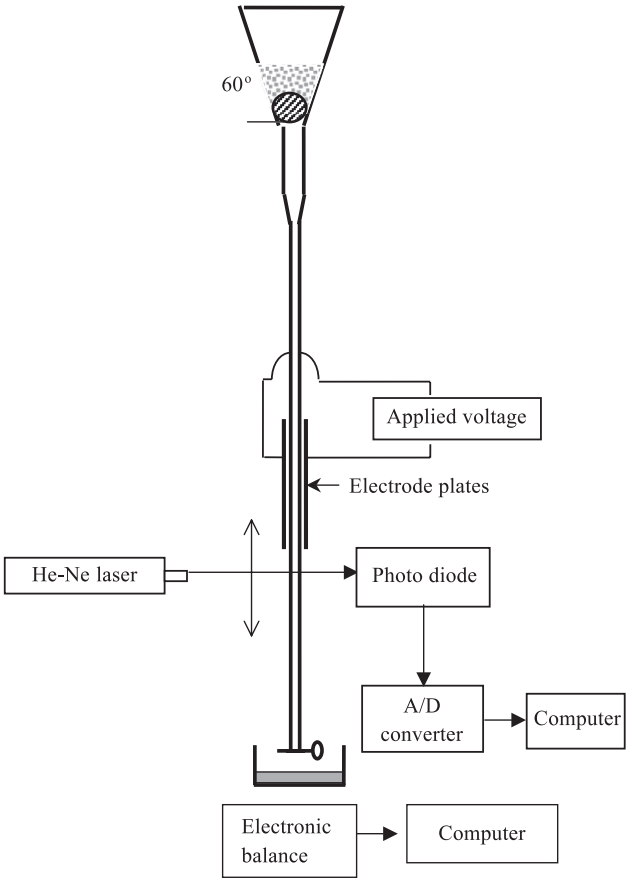

Fig. 1. Schematic of the experiment.

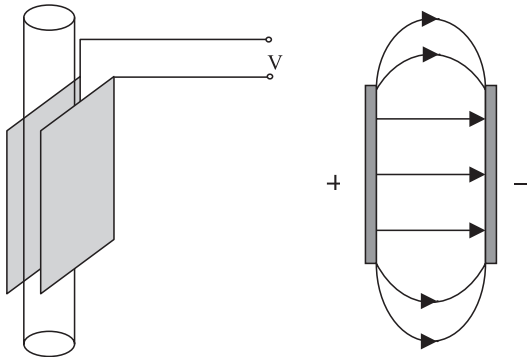

Fig. 2. The pair of electrode plates placed outside of the glass pipe. The field is inhomogeneous near the two ends of the plates as shown.

average diameters $d = 0.25$ mm and $d = 0.35$ mm, are used. Although nickel particles are metallic, they are covered with a thin film of oxide after exposed in air for a long time. The particles are thus electrically insulated from each other. They are filled into a glass hopper joined by a short tube of 4 cm long with inner diameter of 10 mm. Bottom end of the tube converted gradually to a thin pipe of length 10 cm and inner diameter D of 4 mm. Two parallel flat copper electrodes 4.4 mm apart, 10 mm in height and 12 mm in width, are attached to the outside walls of the glass pipe as shown in Fig. 2. By measuring the electric current through the system with and without the granules, we notice that the average local field E_L is less than 1/10 of the external electric field due to the insulation of the glass pipe. We attach the electrodes outside the glass pipe rather than inside for the convenience in handling, for preventing the electric breakdown and for its simplest configuration for basic studies. A 50 Hz ac electric voltage V is applied across the electrodes. The granular flow is initiated by pulling a stopper inserted at the outlet of the hopper. A weighing sensor with sensitivity of 0.02 g and recording rate of 0.02 s is applied at the bottom of the pipe. By measuring the granular mass at each desired electric voltage, the dependence of flow rate vs. voltage can be obtained. When altering the electric voltage from 0 kV to a higher value, a slope difference of the outflow mass $M(t)$ measured as a function of time t can be seen. It provides a direct indication that the granular flow can be retarded by electric field.

During the experiments, the humidity is maintained at 47–55%. This is one of our efforts to reduce the static electric caused by low humidity and, at the same time, to prevent the formation of particle aggregations due to high humidity.

The power spectrum of the outflow density fluctuation is often a subject of much concern. When particles are discharged freely, the density fluctuation shall be dominated by white noise. With no external field the falling particles may be strongly affected by the interstitial air, the power spectrum follows the $1/f^{\alpha}$ law [8]. Here we measure the

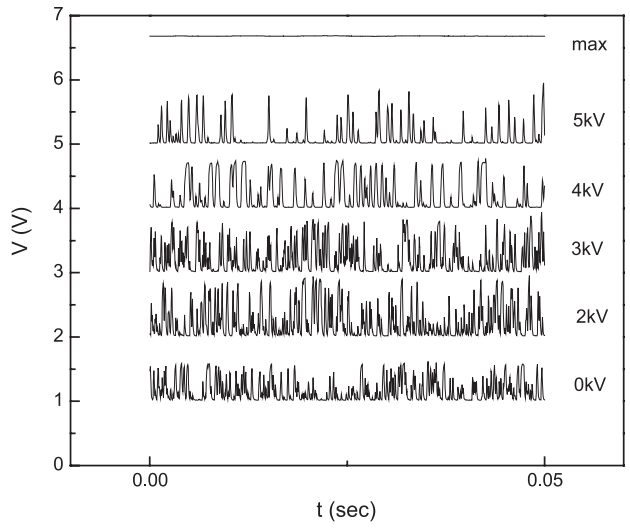

Fig. 3. The transmission signal of the laser light at different electric voltages. The top line is the recorded signal when light is passing through the pipe with no flow particles.

power spectrum of the outflow density fluctuation after the flow passes the electric field. The transmission light of an He–Ne laser beam (wavelength of 632.8 nm), at a position 1 cm lower than the low end of the electrode, passing through the flow is detected by a photodiode. The signal from the photodiode is fed through an A/D converter to a PC. The maximum sampling speed of the A/D converter is 5 MHz. The transmission signal is recorded as shown in Fig. 3. Data of signal recorded at each electric field of external voltage from 0 to 5 kV is shifted by 1 V in Fig. 3. The power spectra of the transmitted light signal are shown in Fig. 4. It is seen that amplitudes of the low frequency components of the spectra do not change much. However, the high frequency components are suppressed more at high voltage. This may be because that the major contribution of the high frequency components is provided by the movements of individual particles. When aggregation occurs, the

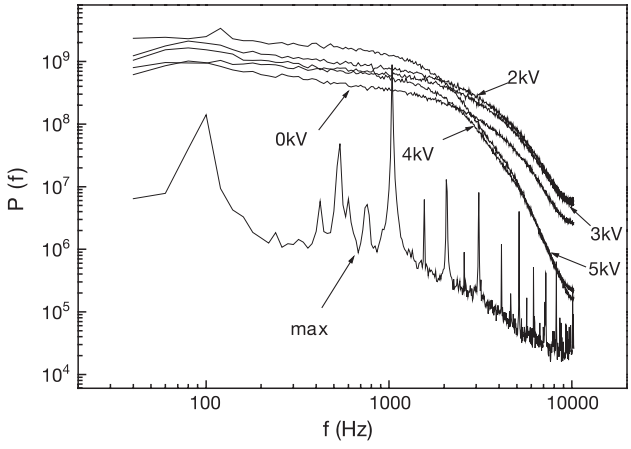

Fig. 4. The power spectra of the laser transmission through the flow at a position 1 cm lower than electrodes at different voltages.

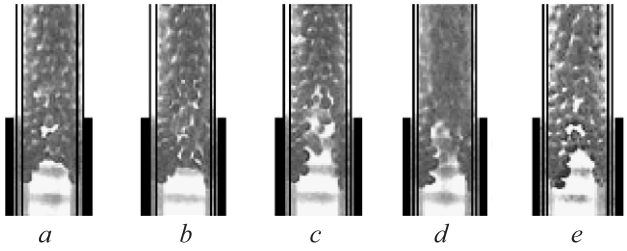

Fig. 5. The unstable arch formed near the top of the electrodes at a high voltage, $V=3$ kV. Pictures a to e were taken at a time sequence in an interval of 0.08 s. The horizontal scale bars are 1 mm apart from each other.

fluctuations caused by movements of individual particles are reduced and therefore suppress the high frequency components. The critical voltage in this case lies in between 3 and 4 kV.

From video images, we can also see that an unstable arch is formed across the pipe near the top edge of the electrodes at $V>V_1$, as shown in Fig. 5. The arch interface is broken and rebuilt continuously at a rate of the order of 0.2 s. The intermittent arch slows down the flow of particles above. When the arch is broken, clusters of granules are seen to drop as can be seen in Fig. 5d where the blurred image shows the fast moving breakaway of the clusters. The flow in the pipe therefore becomes intermittent due to the presence of the electric field.

Experimentally, the initial condition of the flow to be dilute or dense is prepared by two sequences: in the first sequence the flow is initiated after V is set at a fixed value in the range of 0 V–4.8 kV, at an interval of 0.2 kV. The free flow dropping from the hopper outlet passes through the electrodes and the flow rate is affected by the field only when the voltage is above a voltage V_1 as shown in Fig. 6. We find that the flow rate drops abruptly when at this critical voltage and the flow transforms from dilute to dense. To create a dense flow, we

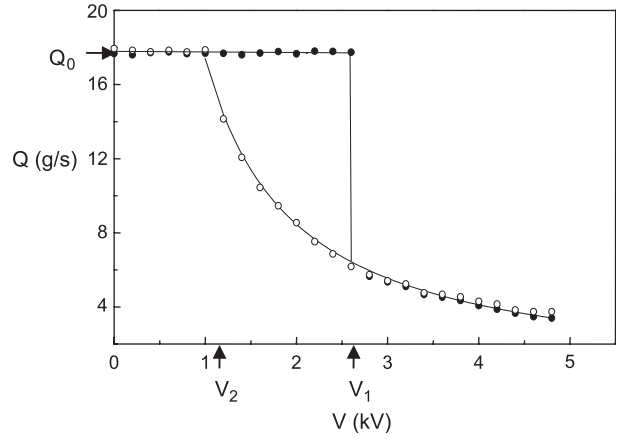

Fig. 6. Dependence of flow rate Q on the voltage V. The solid (open) dots represent the data points obtained from the first (second) sequence experiments. The curved solid line is fitted by $Q=16.9V^{-1}$. The horizontal line is drawn to guide the eye.

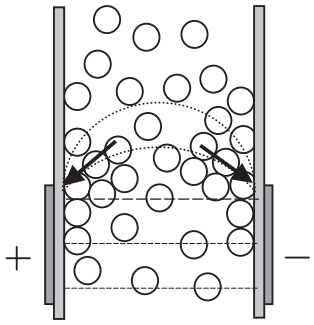

Fig. 7. Sketch of the force acting on particles due to the field gradient near the top of the electrodes. Dashed lines indicate electric lines of force in between electrodes.

first apply a voltage $V=4.8$ kV to the flow. After the flow is initiated and reaches a steady dense flow state, we decrease the V from 4.8 kV to a desired voltage in the range of 0–4.8 kV and record the flow rate. The $Q(V)$ curve of the dense flow is different from the curve obtained from the first sequence where the dilute flow is first initiated. For the dense flow, the $Q(V)$ curve increases monotonically with no sudden jump when decreasing V until it reaches the inflow rate Q_0 at a voltage V_2. The dense flow rate decreases continuously with increasing voltage agreeing with Ghadiri et al.'s [11] result of the dense-phase flow when controlled by the "electromechanical valve". In their case, the applied field is parallel to the flow direction, while we apply a horizontal field to a vertical flow.

3. Particle interaction in electric field

The surface oxidized nickel particles are polarized in the electric field. The induced dipole can be expressed as $\vec{p}=4\pi\varepsilon_0 R^3\vec{E}$, where R is the radius of the particles. The force $\vec{f}_{ij}$ between two induced dipoles p_i and p_j, when particles are not in contact as in dilute flow case, is written as

$$\vec{f}_{ij}=\frac{3}{4\pi\varepsilon_0}\frac{\vec{p}_i\vec{p}_j(1-3\cos\theta\cos\theta)}{|r_{ij}|^4}\hat{r}_{ij}, \quad (1)$$

where θ is the angle between two dipoles i and j. From the above equation, it can be seen that two particles attract each other when $\cos\theta>\sqrt{3}/3$, and repel otherwise. Dipole approximation does not hold when particles are too close to each other that separation $s\approx$ particle diameter d. The attraction increases nonlinearly when $s\approx d$.

Considering only dipole interaction, the force acting on the polarized particle in an inhomogeneous electric field can be expressed as

$$\vec{f}=-\nabla(-\vec{p}\,\vec{E})=4\pi\varepsilon_0 R^3\nabla E^2. \quad (2)$$

When the electric field is high enough, i.e. the interaction is comparable to the kinetic energy of the falling particles, the particles will be dragged by the field gradient. The threshold field strength E_1 is 7×10^2 kV/m (corresponds to external voltage of 3.1 kV) when the force balances the particle's weight if we only consider the force due to dipole interaction as given in Eqs. (1) and (2). In reality, the local field E_L is at least one order of magnitude smaller than the external field due to the voltage drop on the dielectric glass pipe. At such a low E_L the particle aggregation occurs due to the field-enhanced nonlinearly increasing particle attraction at $s\approx d$.

Above a threshold voltage, particles converge to the sidewall near the top of the electrodes shown in Fig. 7. The arrows in Fig. 7 represent the direction of the dragging force. This force against the sidewall induces a friction between particle and wall, which will reduce the velocity of particles along the wall. The interaction between polarized particles attracts them to move closer to each other, and enlarges E_L (E_L is proportional to V) between particles. The enhancement of local field between particles will further increase their mutual induction and cause particles to interact with each other and aggregation occurs. (When two particles are in contact, the increased force between them due to this enhanced electric field corresponds to the electroclamping effect discussed by Ghadiri et al. [10,11].) This positive-feedback effect, we believe, is the major contribution that causes the flow rate to reduce dramatically at the critical voltage V_1.

The flow rate keeps constant for dilute flow before the critical voltage can be explained as follows. The particle falling velocity is retarded by the electric field when they enter the field area. The velocity becomes a function of

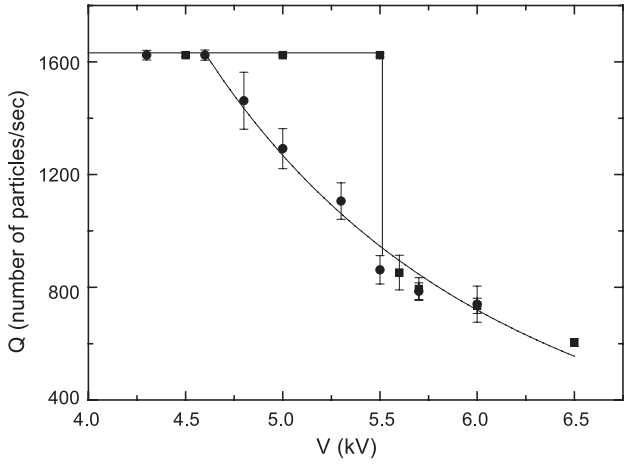

Fig. 8. Simulation result of $Q(V)$ curve by a two-dimensional MD model. The solid (open) dots represent data obtained from the first (second) sequence, corresponding to an initial dilute (dense) flow. The solid lines are drawn to guide the eye.

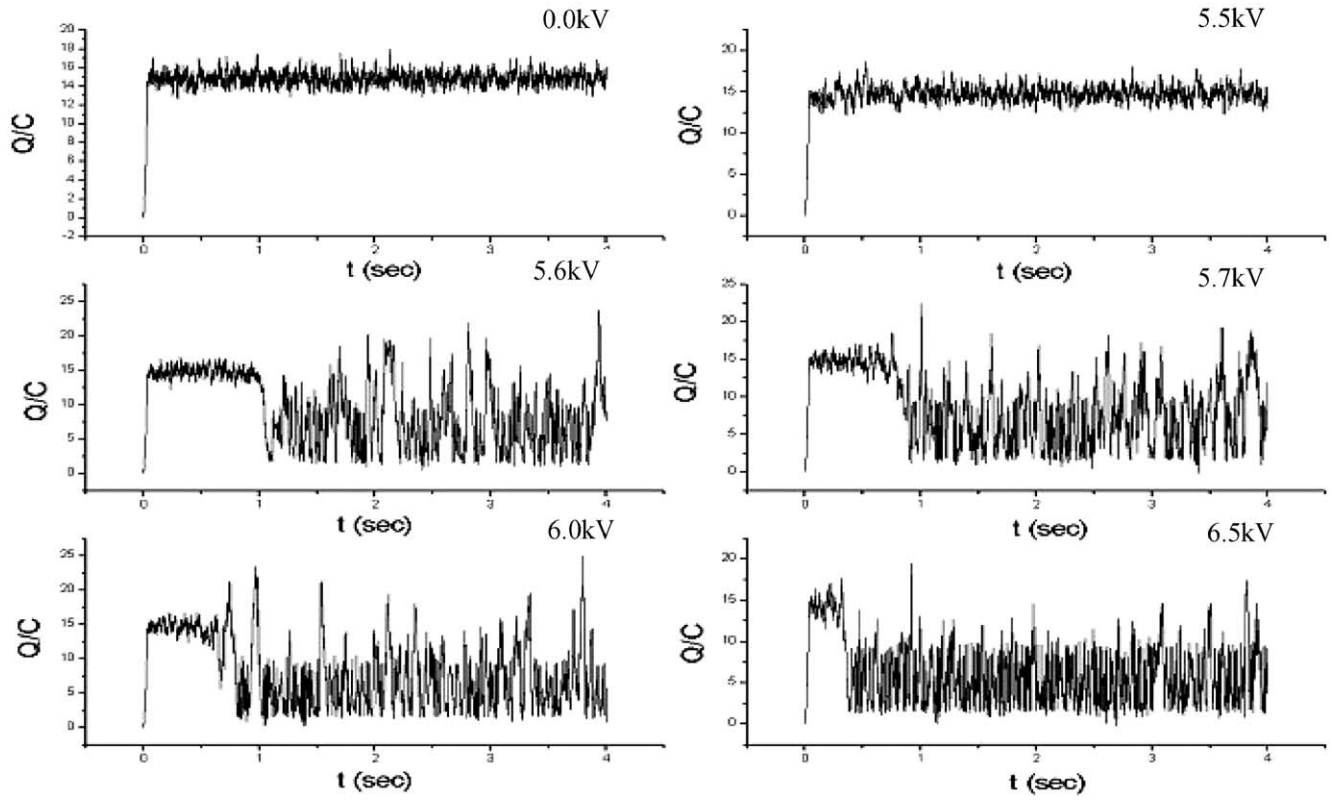

Fig. 9. Simulation results of $Q(t)$ at different voltages. At voltages above the critical voltage, flow transition from dilute to dense occurs. When it becomes dense flow, intermittence of the flow is seen and flow rate drops abruptly.

the local field E_L, which is in turn proportional to V. When $V<V_1$, the slowdown of the particles in the field is accompanied by an increase of the particles density, and makes the flow rate invariant with V. When $V>V_1$ (when $s=d$), the particle density reaches a maximum and the slowdown of the particles therefore reduce the flow rate because the rate $Q=v\rho$, where v is the mean particle velocity and r the density of the flow.

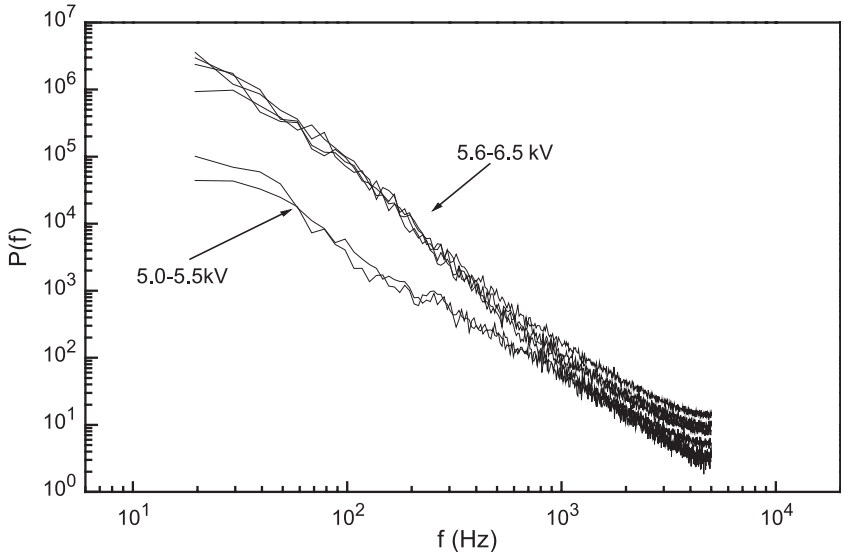

Fig. 10. Simulation results of the power spectra of the density fluctuation frequencies. The spectrum $P(f) \sim f^{-\alpha}$ with $\alpha \approx 1.9$ when V is in the range of 5.0–5.5 kV, and $\alpha \approx 2.9$ when V is above 5.5 kV.

4. Two-dimensional molecular dynamics simulation

A two-dimensional computer simulation based on molecular dynamics (MD) model [17], in which the collision between particles, the interaction between polarized particles, the force imposed on the polarized particles by the electric field, and the gravitational force are considered. The interacting force at contact obeys the following equations:

$$F^{\mathrm{n}}_{j\to i} = K_{\mathrm{h}}(R_i + R_j - |\overrightarrow{r_{ij}}|)^{3/2} - K_{\mathrm{d}} m_{\mathrm{eff}}(\overrightarrow{v_{ij}}\hat{r}_{ij}), \tag{3}$$

where $F^{\mathrm{n}}_{j\to i}$ represents the normal force. The first term is the Hertizan elastic force, where R_i, R_j are the radii of particle i and j; $\overrightarrow{r_{ij}} = \overrightarrow{r_i} - \overrightarrow{r_j}$($\overrightarrow{r_i}$, $\overrightarrow{r_j}$ are the positions of the center of particles i and j) and K_{h} is the elastic constant of the material. The second term is the damping term, where $\overrightarrow{v_{ij}} = \overrightarrow{v_i} - \overrightarrow{v_j}$($\overrightarrow{v_i}$, $\overrightarrow{v_j}$ are the velocity of the particles i and j), K_{d} is the normal dissipation coefficient, and m_{eff} is the effective mass, $m_i m_j/(m_i + m_j)$.

The shear component force $F^{\mathrm{s}}_{j\to i}$ can be written as follows:

$$F^{\mathrm{s}}_{j\to i} = -K_{\mathrm{s}} m_{\mathrm{eff}}(\overrightarrow{v_{ij}}\hat{s}_{ij}) - \mathrm{sgn}\left(\overrightarrow{l}\right)\min(K_{\mathrm{l}}|\overrightarrow{l}|, \mu|\overrightarrow{F}^{\mathrm{n}}_{j\to i}|), \tag{4}$$

where the first term is a damping term, the second term is a term considering the static friction, in which μ is the static friction coefficient, l is the total shear displacement during the contact, and K_{l} is the elastic constant of a virtual spring. When the particle i collides with the wall, we have $m_{\mathrm{eff}} = m_i$ and $R_j = 0$. In our model, we do not yet take rotation into account.

The simulation result of the dependence of flow rate Q upon voltage V is obtained and is shown in Fig. 8. The $Q(V)$ dependence of dilute and dense flows agrees qualitatively with the experimental observation. The intermittence of the flow after the flow transforms from dilute to dense is shown in Fig. 9. Its frequency distribution is analyzed by the power spectrum, which is shown in Fig. 10. It also shows the suppression of high frequency components at $V > V_1$, which agrees with the experimental observation of particle aggregation at high voltages.

5. Conclusion

In conclusion, the effect of an applied local, horizontal ac electric field to the flow of nickel particles in a vertical pipe is studied experimentally. It is found that the field is able to retard the flow, and the effect of the field to the flow rate depends upon the initial condition of the flow. For dilute flow, the flow rate does not change until V is greater than a critical voltage V_1, at which dilute flow transforms to dense flow. The flow rate is then retarded by the electric field when V is higher than V_1. The value V_1 depends upon the flow density, which can be changed by changing the position of the electrode plates along the pipe. When the electrodes are placed further away from the hopper, flow density is smaller, and the critical voltage V_1 is higher. Results on the density dependence of the critical voltage will be further studied. For dense flow, the field retards the flow rate monotonically when the voltage is higher than a different voltage V_2, while $V_2 < V_1$. The value V_2 is a cutoff voltage determined by the inflow rate.

The transition of the flow from dilute to dense induced by the electric field is explained to be due to the particle convergence and aggregation near the top of the electrodes where the field gradient is greatest. These aggregations slide down slowly along the inner sidewalls near the electrodes and are the major cause of the retardation. The positive feedback of the local field $E_{\mathrm{L}}(r)$ is believed to be the reason of the sudden drop in flow rate at the transition from dilute to dense. The simulation results confirm the aggregation and the intermittence of the flow being affected by the electric field.

Nomenclature

d	average diameter of particles
D	inner diameter of the pipe
E_1	threshold field strength
E_{L}	average local field
$\overrightarrow{f_{ij}}$	force between two induced dipoles p_i and p_j
K_{d}	normal dissipation coefficient
K_{h}	elastic constant of the material
K_{s}	shear dissipation coefficient
K_{l}	elastic constant of a virtual spring
l	total shear displacement during the contact
m_{eff}	effective mass
$\overrightarrow{p}$	induced electric dipole
Q	flow rate
Q_0	inflow rate
$\overrightarrow{r_i}$, $\overrightarrow{r_j}$	positions of the center of particles i and j
R_i, R_j	radii of particle i and j
s	distance between the center of mass of two particles
v	mean particle velocity
V	applied electric voltage
V_1	critical voltage
$M(t)$	outflow mass
ρ	density of the flow
μ	static friction coefficient

Acknowledgements

This research is supported by the State Key Program for basic research of Chinese National Science Foundation.

References

[1] J. Rajchenbach, Adv. Phys. 49 (2000) 229.
[2] L.P. Kadanoff, Rev. Mod. Phys. 71 (1999) 435;
P.G. de Gennes, Rev. Mod. Phys. 71 (1999) S374;
H.M. Jaeger, S.R. Nagel, R.P. Behringer, Rev. Mod. Phys. 68 (1996) 1259.
[3] H.M. Jaeger, S.R. Nagel, Science 255 (1992) 1523.
[4] T. Raafat, J.P. Hulin, H.J. Herrmann, Phys. Rev., E 53 (1996) 4345.
[5] J.L. Aider, et al., Phys. Rev., E 59 (1999) 778.
[6] S. Horikawa, et al., Physica, A 233 (1996) 699.
[7] A. Nakahara, T. Isoda, Phys. Rev., E 55 (1997) 4264.
[8] O. Moriyama, N. Kuroiwa, M. Matsushita, H. Hayakawa, Phys. Rev. Lett. 80 (1998) 2833.
[9] I.S. Aranson, D. Blair, V.A. Kalatsky, G.W. Crabtree, W.-K. Kwok, V.M. Vinokur, U. Welp, Phys. Rev. Lett. 84 (2000) 3306.
[10] W. Balachandram, D. Hu, M. Ghadiri, S.E. Luw, S.A. Thompson, IEEE Trans. Ind. Appl. 33 (1997) 871;
C. Martin, M. Ghadiri, U. Tuzun, Proceedings of 2nd World Congress Particle Technology, Sept. 19–22, 1990. Soc. Powder Technology, Japan, Kyoto, pp. 182–191.
[11] M. Ghadiri, C.M. Martin, J.E.P. Morgan, R. Clift, Powder Technol. 73 (1992) 21–35;
C.M. Martin, M. Ghadiri, U. Tuzun, B. Formisani, Powder Technol. 65 (1991) 37–49.
[12] C.M. Talbert, et al., IEEE Trans. Ind. Appl. IA-20 (1984) 1220.
[13] P.W. Dletz, J.R. Melcher, Ind. Eng. Chem. Fundam. 17 (1978) 28.
[14] W. Chen, M. Hou, K. Lu, Z. Jiang, L. Lam, Europhys. Lett. 56 (4) (2001) 536–541.
[15] W. Chen, M. Hou, K. Lu, Z. Jiang, L. Lam, Phys. Rev., E 64 (2001) 61305.
[16] W. Chen, M. Hou, K. Lu, Z. Jiang, L. Lam, Appl. Phys. Lett. 80 (12) (2002) 2213.
[17] J. Lee, Phys. Rev., E 49 (1994) 281.